arXiv:1409.6494v1 [cond-mat.stat-mech] 23 Sep 2014

Transverse ratchet effect and superconducting vortices: Simulation and experiment

L Dinis[1], D Perez de Lara[2], E M Gonzalez[2], J V Anguita[3], J M R Parrondo[1] and J L Vicent[2]

Abstract. A transverse ratchet effect has been measured in magnetic/superconducting hybrid films fabricated by electron beam lithography and magnetron sputtering techniques. The samples are Nb films grown on top of an array of Ni nanotriangles. Injecting an ac current parallel to the triangle reflection symmetry axis yields an output dc voltage perpendicular to the current, due to a net motion of flux vortices in the superconductor. The effect is reproduced by numerical simulations of vortices as Langevin particles with realistic parameters. Simulations provide an intuitive picture of the ratchet mechanism, revealing the fundamental role played by the random intrinsic pinning of the superconductor.

PACS numbers: 05.40.-a, 02.30.Yy,74.25.Qt, 85.25.-j

[1] Grupo Interdisciplinar de Sistemas Complejos (GISC) and Departamento de Física Atómica, Nuclear y Molecular. Universidad Complutense de Madrid. E-28040 Madrid, Spain.

[2] Departamento de Física de Materiales. Universidad Complutense de Madrid. E-28040 Madrid, Spain.

[3] Instituto de Microelectrónica de Madrid. Consejo Superior de Investigaciones Científicas. Tres Cantos, E-28760,Spain.

1. Introduction

The study of transport in asymmetric substrates, under the generic name of "ratchet phenomena", has attracted increasing attention in the last years. Ratchets exhibit unexpected transport properties, such as rectification or negative resistance, which can be used to control motion and also to reveal aspects of the underlying dynamics in many physical systems [1, 2]. This is the case of vortex motion in superconductors, where different types of ratchets have been implemented using substrates with asymmetric defects [3].

In ratchets, asymmetry is normally used to rectify an ac signal, but it can also induce other non trivial transport effects. One of these effects is the so-called transverse ratchet, in which an ac force can induce a directed motion *perpendicular* to the force. Several authors have theoretically worked on this topic [4, 5, 6, 7]. Olson-Reichhardt and Reichhardt [8] have studied this effect by numerical simulations of superconducting vortices as Langevin interacting particles. In a recent publication, Gonzalez *et al.* [9] have presented experimental evidence of transverse ratchet in superconducting samples, using non-superconducting triangles embedded in a superconducting film. In the usual ratchet effect configuration the driving current is applied perpendicular to the triangle reflection symmetry axis (tip to base axis) and the output dc voltage signal is measured on the same direction. However, in the case of transverse ratchet, the driven current is applied parallel to the triangle reflection symmetry axis, and the output voltage drop is measured perpendicular to the input current direction, i.e. perpendicular to the triangle reflection symmetry axis. We recall that the voltage drop in one direction probes the vortex motion along the perpendicular direction, as given by the Lorentz force and the Josephson equation [9] (a schematic representation of the transverse setup is shown in figure 1).

In this work we show that this transverse ratchet effect can be modeled in the framework of the Langevin equation in two dimensions (2D), taking into account that we are dealing with an adiabatic ratchet effect of interacting particles [10]. The crucial point is the interplay between two pinning potentials: i) intrinsic and random pinning potentials, due to the structural defects present in the superconducting films, ii) artificial periodic ratchet pinning potentials, due to the array of non superconducting nanostructures embedded in the superconducting films. This approach is able to reproduce the sign and magnitude of the experimental data, with realistic values of all the parameters involved in the simulation.

2. Experimental method

The samples are superconducting/magnetic hybrids; i.e. Nb films grown on top of arrays of Ni nanotriangles which are fabricated on Si (100) substrates. These samples are obtained following several steps with different techniques. The first one is e-beam writing of the nanotriangles on a polymethyl methacrylate (PMMA) resist covering the

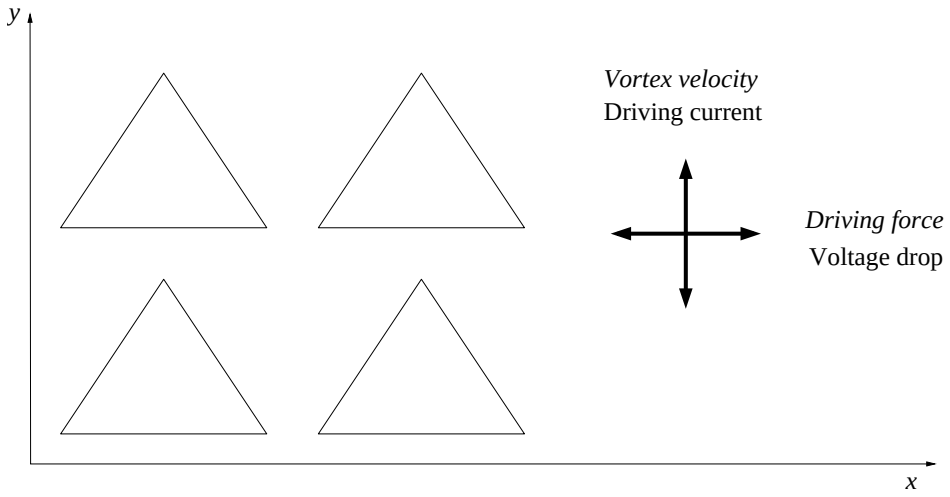

Figure 1. Transverse ratchet configuration.

Si (100) substrate, next developing using methyl isobutyl ketone : isopropyl alcohol (1:3) during 15 seconds, and magnetron sputtering deposition of Ni. Once lift-off is performed and the resist is removed, only nanometric Ni triangles remain on top of the substrate, which is then covered by a thin film of Nb, also by magnetron sputtering technique. The thicknesses are always the same, for Ni (triangles height) 40 nm, and 100 nm for the Nb film. The nanotriangles side is around 600 nm. The array period is 770 nm $\times$ 750 nm. Samples were lithographed with a cross-shaped bridge (40 μm wide) using standard optical lithography and reactive ion etching techniques for magnetotransport measurements. This cross-shaped bridge allows injecting a transport current and measuring voltage drops along two perpendicular directions. This guarantees that the only asymmetry in the experimental layout is coming from the Ni triangular traps. Magnetotransport measurements were carried out in a commercial liquid He cryostat provided with a superconducting magnet and a variable temperature insert. The magnetic field, which creates the vortex lattice, is applied perpendicular to the film. The magnetic properties of these arrays of Ni triangles have been already published [11]. The temperature is kept constant and close to the superconducting critical temperature, which is around 8.7 K in our samples. The measurements have been done with a frequency of the ac applied current of 10 kHz. The experimental configuration is Hall-like, the injected ac current is applied parallel to the triangle reflection symmetry axis (tip to base axis) and the output voltage is recorded perpendicular to this axis. This type of measurements could yield experimental artefacts due, for instance, to misalignment of the potential contacts. In the related literature one can find well known experimental methods to avoid these unwanted effects for all kind of unpatterned [12] or patterned [13] samples. In our case, the experimental signal coming from these effects is much smaller than the transverse ratchet effect signal and the possible contribution to the experimental data could be neglected as was reported in [9].

Finally, close to critical temperature [14] magnetoresistance of superconducting thin films with periodic arrays of pinning centers show minima when the vortex lattice matches the unit cell of the array [15]. This geometric matching occurs when the vortex density is an integer multiple of the pinning center density, hence the number n of vortices per array unit cell can be known by simple inspection of the magnetoresistance curves, in which the first minimum corresponds to one vortex per unit cell, the second minimum to two vortices per unit cell, and so on. Therefore, changing the applied magnetic field we can select the number of vortices per array unit cell.

The transverse ratchet effect has been observed for different values of n, as shown in Fig. 3. Firstly, we proceed to describe the numerical simulations and then we discuss the results.

3. Numerical simulations

We have performed extensive numerical simulations of vortices as a set of 2D interacting, overdamped Brownian particles in the Langevin approach. This type of simulations have been used to study rectification, current reversal and lattice configurations effects [8, 16, 17]. Transverse vortex rectification has been previously analyzed by Olson-Reichhardt, and Reichhardt [8] and Savel'ev *et al.* [6] using similar simulations. However, our experimental results differ from these simulations.

Even though random intrinsic pinning effects in Nb and type-II superconductors without periodic pinning traps have been widely discussed [18], Langevin type simulations of experimental vortex ratchet systems usually disregard the effect of intrinsic pinning centers [8, 16, 17, 19, 20, 21, 22]. As pointed out by A. Kolton [7], pinning defects may have a strong influence in the transversal ratchet effect. In our simulations Nb intrinsic pinning is taken into account as a random distribution of potential wells, and as we will see later, the disorder induced by the intrinsic pinning in the vortex lattice plays a fundamental role in the transverse ratchet effect.

Langevin equation for the position $\mathbf{r}_i$ of the i-th vortex reads:

$$\eta\dot{\mathbf{r}}_i(t) = -\sum_{j\neq i}\vec{\nabla}_i U_{vv}\left(|\mathbf{r}_i-\mathbf{r}_j|\right) - \vec{\nabla}_i V_{tp}(\mathbf{r}_i) - \vec{\nabla}_i V_{ip}(\mathbf{r}_i) + \mathbf{F}_{\rm ext}(t) + \mathbf{\Gamma}_i(t) \quad (1)$$

where η is the viscosity, $U_{vv}(r)$ is the interaction potential between vortices, $\mathbf{F}_i^{tp}(\mathbf{r}_i) = -\vec{\nabla}_i V_{tp}(\mathbf{r}_i)$ the force due to Ni triangular pinning traps, $\mathbf{F}_i^{ip}(\mathbf{r_i}) = -\vec{\nabla}_i V_{ip}(\mathbf{r}_i)$ the force due to randomly distributed pinning centers present in the Nb sample, $\mathbf{F}_{\rm ext}(t)$ the external force due to the applied current, and $\mathbf{\Gamma}_i(t)$ are white Gaussian noises accounting for thermal fluctuations:

$$\langle \mathbf{\Gamma}_i(t)\cdot\mathbf{\Gamma}_j(t')\rangle = 4kT\eta\delta_{ij}\delta(t-t'). \quad (2)$$

For the vortex interaction potential, we have used [23]:

$$U_{vv}(r) = \frac{\phi_0^2 d}{2\pi\mu_0\lambda^2}K_0\left(\frac{r}{\lambda}\right) \quad (3)$$

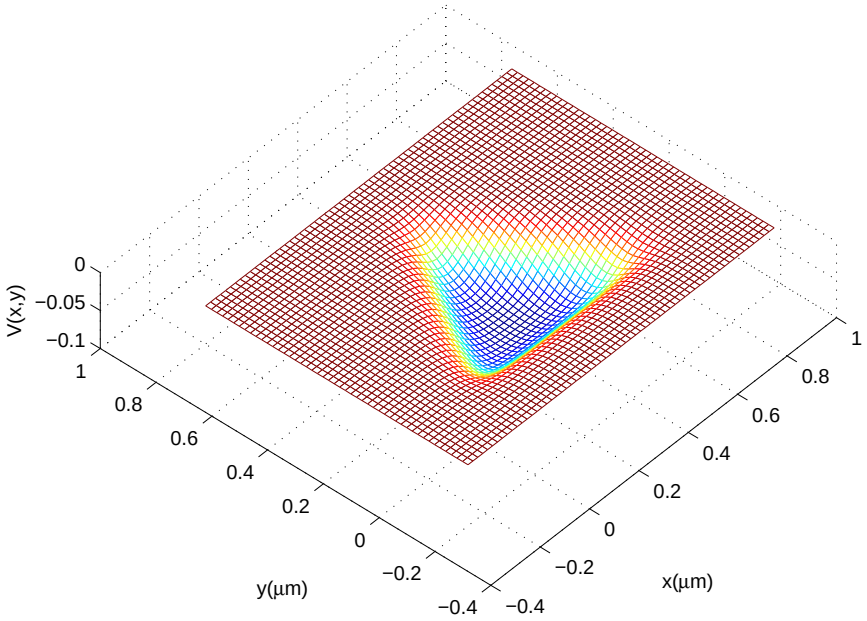

Figure 2. Potential used for vortex-triangle interaction.

where $\phi_0 = h/(2e)$ is the quantum of flux, μ_0 is the magnetic permeability of vacuum, K_0 is the zeroth-order modified Bessel function, λ is the penetration depth of the material, and d is sample thickness.

For the friction coefficient η, we have used Bardeen-Stephen contribution to vortex viscosity per unit length giving $\eta = \phi_0^2 d/2\pi\xi^2\rho_n$, where d is the sample thickness, ξ the vortex coherence length and ρ_n is normal state resistivity for Nb.

The external force is sinusoidal as in the experiment, with the same amplitude but different frequency. Friction coefficient and vortex interaction strength set the appropriate time scale for simulation, and unfortunately, the small time step required ($\Delta t = 2 \times 10^{-6}\mu$s) prevents us from using the experimental value of applied force frequency of 10kHz. However, experiments show that the system is adiabatic and the result does not depend on signal frequency, which allows us to use an adiabatic approximation as in [17]. Finally, we have compared adiabatic simulations with those using an AC signal of 5MHz showing that this is a sufficiently small frequency as to yield the same results (not shown). For the rest of the simulations we have used a 5MHz signal because this slightly simplifies data analysis by avoiding numerical computations of the adiabatic integral.

The interaction between vortices and the triangular Ni pinning wells is modeled by a potential V_{tp} in the shape of a triangle and with a smooth hyperbolic tangent profile and rounded vertices and intensity V_{tp0}, as depicted in figure 2.

Intrinsic pinning defects have been simulated as a series of potential wells randomly distributed across the sample and in the shape of paraboloids truncated at radius r_d.

Magnitude	Symbol	Value
Friction coefficient * [29]	η	6×10^{-5} pNμs/μm
Penetration length * [30]	λ	0.320 μm
Coherence length *	ξ	0.090 μm
Sample thickness *	d	0.100 μm
Temperature *	T	8.3 K
Triangular pinning **	$V_{\rm tp0}$	0.08 pNμm
Intrinsic pinning **	$V_{\rm def}$	0.015 pNμm
Defect density **	$\rho_{\rm eff}$	14.5 μm^{-2}

Table 1. Numerical values used in simulations in units pN, μm, μs and K. *: Experimental values. **: Values that have been adjusted to reproduce experimental data behaviour.

Thus, the interaction potential of vortex i with a defect in position $\mathbf{r_c}$ is

$$V_{ip}(\mathbf{r}_i) = -V_{\rm def} + \frac{V_{\rm def}}{r_d^2}(\mathbf{r}_i - \mathbf{r}_c)^2, \text{ if } |\mathbf{r}_i - \mathbf{r}_c| < r_d \tag{4}$$

and zero otherwise, where $V_{\rm def}$ represents the intensity of the intrinsic pinning potential. Following [24, 25, 26, 27, 28], we have chosen the size of the defect as the size of the vortex core $r_d = \xi$, which corresponds to point defects interacting with the core of the flux quantum. If the density of pinning defects is sufficiently high as it is in Nb samples the overlapping pinning centers will lead to a diffuse potential or "pin-scape" which can be described by a much lower effective pinning density and certain amplitude [24]. Only a small fraction of the resulting wells will have an amplitude large enough to produce appreciable pinning, the majority of them overlap producing a low amplitude wriggling in the pinning potential. This effective density has been chosen large enough so that the defects produce lattice distortion, but not too large so that computer simulation time remains below a reasonable limit.

Table 1 presents a summary of numerical values used in simulation.

Experimental and simulation results are represented in figure 3. Simulations and experiment data show similar behavior. Several differences can be observed though. For instance, simulated vortex velocity does not decay with force as fast as in the experimental curves. In the case of the simulations, the decay is that of an adiabatic system where the velocity is expected to decay slowly, as the inverse of the square root of the applied peak force intensity. This is due to the fact that even for very high peak forces, the sinusoidal applied force covers small values of the force for a short interval. This is however not observed in the experimental data although the system is known to be adiabatic with respect to the applied force frequency [3, 10]. At high enough driving forces, a vortex velocity threshold is found in the experiments above which the interaction between the moving vortex lattice and the ordered array is very weak, if

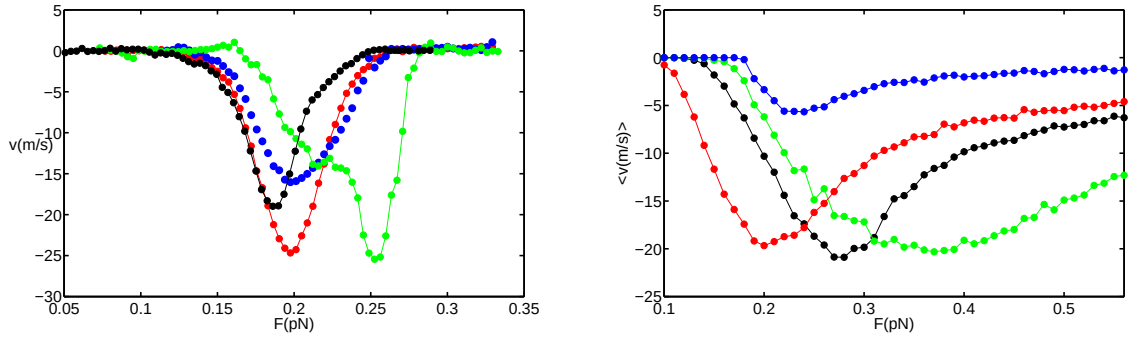

Figure 3. *Left:* Measured average vortex speed versus amplitude of applied force, for applied magnetic field $H = 64$Oe ($n = 2$) (green), $H = 96$Oe ($n = 3$) (black), $H = 128$ Oe ($n = 4$) (blue) and $H = 176$ Oe ($n = 6$)(red), $T/T_c = 0.98$. *Right*: Simulation results, average vortex speed versus amplitude of applied force, for $n = 2$ (green), $n = 3$ (black), $n = 4$ (blue) and $n = 6$ (red) vortices per unit cell. The lines joining the dots is only a guide for the eye.

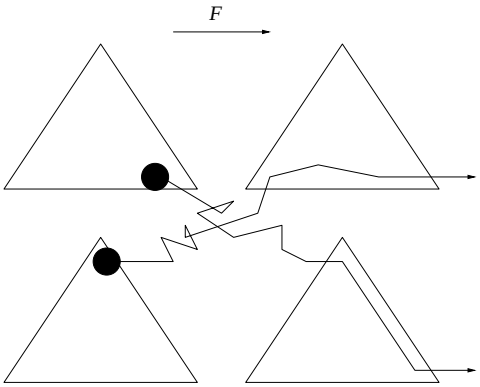

Figure 4. Sketch of rectification mechanism (see text for discussion).

any, and commensurability effects are suppressed as was reported by Velez et al. [31]. Nevertheless, we point out that the sign of the current is correctly reproduced by our simulations, which also agree with the order of magnitude of velocities and applied force.

4. Discussion: rectification mechanism

The mechanism for transverse rectification is depicted in figure 4 (see also supplementary material) and can be stated as follows:

(i) Fluctuations may take a vortex to a neighbouring row of triangles.

(ii) If a vortex enters a triangle by its tip (downward motion in figure 4) it may be carried further down parallel to the side of the triangle by the combination of the horizontal force and the triangular potential. If the vortex enters the triangle at its base (upward motion in figure 4), the external force and the triangle potential keep it close to the triangle base. Thus, downward fluctuations are promoted or favoured, ratcheting the particles down and yielding a negative particle current.

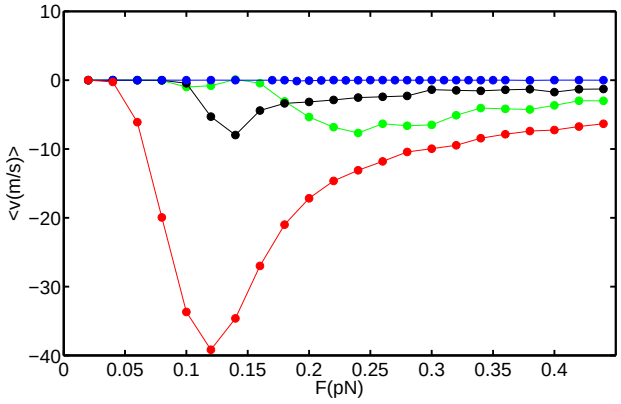

Figure 5. Simulation results, average vortex speed versus amplitude of applied force in the absence of intrinsic pinning, for $n = 2$ (green), $n = 3$ (black), $n = 4$ (blue) and $n = 6$ (red) vortices per unit cell. The line joining the points is only a guide for the eye.

As explained, fluctuations are essential for this mechanism, the source of these usually being the temperature in most systems. However, the temperature in our experimental system is too low to provide fluctuations of sufficient amplitude. As previously stated, the role of temperature fluctuations can also be played by a random distribution of pinning centers which may add the needed stochasticity to vortex motion.

As expected, removing the pinning centers from simulations makes the transverse signal disappear for $n = 4$ and drastically reduces the signal for $n = 2$ and $n = 3$. For $n = 4$ and without intrinsic pinning disorder the Abrikosov lattice formed by the vortices approximately matches the triangle square lattice, forming a well ordered almost triangular lattice, as explained and depicted in [17]. When pulled horizontally, vortices move in almost perfect order from one column to the next, yielding a vanishing vertical current, as shown in figure 5 (see also supplementary material). For $n = 2$, the vortex lattice is not perfectly ordered even in the absence of intrinsic pinning disorder, presenting some interstitial vortices, a small part of the triangles trapping just one vortex or three. This disorder is enough to provide a small transversal signal as shown also in figure 5, however, the addition of pinning disorder clearly enhances the signal, as also happens for $n = 3$.

Finally, the effect or pinning disorder is the opposite for $n = 6$, where the vortex interaction is stronger and matching between the vortex and the array of triangles is worse in the absence of intrinsic disorder. In this case, adding intrinsic pinning merely increases the overall pinning and the movement of the vortices is slower, giving less signal.

Supplementary multimedia material allows the reader to compare simulations with or without intrinsic pinning disorder and inspect the mechanism behind rectification.

5. Conclusions

In summary, hybrids of superconducting films with periodic asymmetric nanotriangles show transverse ratchet effect, i.e. injecting an ac current parallel to the reflection symmetry axis yields a dc output voltage in the perpendicular direction. This effect can be modelled in the framework of Langevin equation for interacting particles in 2 dimensions. The simulations provide an intuitive mechanism for the observed transverse rectification of vortices. Moreover, we have shown that intrinsic random pinning is necessary to reproduce the experimental results. The role played by the intrinsic pinning is smeared out increasing the number of vortices.

Acknowledgments

We acknowledge funding support by Spanish Ministerio de Ciencia e Innovación grants NAN04-09087 and MOSAICO, FIS2005-07392, Consolider CSD2007-00010, FIS2008-06249 (Grupo Consolidado) and CAM grant S-0505/ESP/0337, and Fondo Social Europeo. Computer simulations of this work were performed at the "Cluster de cálculo para Técnicas Físicas"at UCM, funded in part by UE-FEDER program and in part by UCM.

References

[1] Reimann P, 2002, *Phys. Rep.* **361** 57
[2] Linke H (Ed.) 2002 Special issue on Ratchets and Brownian Motors: basic, experiments and applications. Appl. Phys. A 55, vol. 2
[3] Villegas J E, Savel'ev S, Nori F, González E M, Anguita J V, Garcia R and Vicent J L 2003 *Science* **302** 1188
[4] Derenyi I and Astumian R D 1988 *Phys. Rev.* E **58** 1
[5] Bier M, Kostur M, Derenyi I and Astumian R D 2000 *Phys. Rev.* E **61** 7184
[6] Savel'ev S, Misko V, Marchesoni F and Nori F 2005 *Phys. Rev.* B **71** 214303
[7] Kolton A B 2007 *Phys. Rev.* B **75** 020201(R)
[8] Reichhardt C J O and Reichhardt C 2005 *Physica* C **432** 125
[9] González E M, Nunez N O, Anguita J V and Vicent J L 2007 *Appl. Phys. Lett.* **91** 062505
[10] Villegas J E, González E M, Gonzalez M P, Anguita J V, and Vicent J L 2005 *Phys. Rev.* B **71** 024519
[11] Jaafar M, Yanes R, Asenjo A, Chubykalo-Fesenko O, Vazquez M, Gonzalez E M, Vicent J L 2008 Nanotechnology **19**, 285717
[12] Colino J, Gonzalez M A, Martin J I, Velez M, Oyola D, Prieto P and Vicent J L 1994 *Phys. Rev.* B **49** 3496
[13] Crusellas M A, Fontcuberta J, Pinol S, Cagigal M and Vicent J L 1993 *Physica* C **210** 221
[14] Martin J I, Velez M, Hoffmann A, Schuller I K, and Vicent J L 2002 *Phys. Rev.* B **62**, 9110
[15] Martin J I, Velez M, Nogues J, and Schuller I K 1997 *Phys. Rev. Lett.* **79** 1929
[16] Dinis L, González E M, Anguita J V, Parrondo J M R and Vicent J L 2007 *Phys. Rev.* B **76** 212507
[17] Dinis L, González E M, Anguita J V, Parrondo J M R and Vicent J L 2007 *New J. Phys.* **9** 366
[18] Campbell A M and Evetts J E 1972 *Adv. Phys.* **21** 199
[19] de Souza Silva C C, Van de Vondel J, Morelle M and Moshchalkov V V 2006 **Nature 440** 651

[20] Lu Q, Olson Reichhardt C J and Reichhardt C 2007 *Phys. Rev.* B **75** 054502
[21] Zhu B Y, Van Look L, Moshchalkov V V, Marchesoni F and Nori F 2003 *Physica* E **18** 322
[22] Reichhardt C, Olson C J and Nori F 1998 *Phys. Rev.* B **57** 7937
[23] Tinkham M 1996 Introduction to Superconductivity (New York: McGraw-Hill) p. 154
[24] Jensen H J, Brechet Y and Brass A 1988 *J. Low Temp. Phys.*, **74** 293
[25] Dong J 1993 *J. Phys.: Condens. Matter* **5** 3359
[26] Wang Z D, Ho K M, Dong J and Zhu J 1995 *Phys. Rev.* B **51** 6119
[27] Wang Z D and Ho K M 1996 *Z. Phys.* B **100** 547
[28] Zhu B Y 1997 *Physica* C **276** 309
[29] Bardeen J and Stephen M J 1965 *Phys. Rev.* **140** A1197
[30] Hake R R 1967 *Phys. Rev.* **158** 356
[31] Velez M, Jaque D, Martín J I, Guinea F, and Vicent JL 2002 *Phys. Rev.* B **65**, 094509